Accurate Modeling of Microwave Structures Using Variable-Fidelity Response Features

Slawomir Koziel[†], *Senior Member, IEEE*, and John W. Bandler[‡], *Life Fellow, IEEE*

† School of Science and Engineering, Reykjavik University, 101 Reykjavik, Iceland
‡ Department of Electrical and Computer Eng., McMaster University, Hamilton, ON, Canada L8S 4K1

Abstract — This paper describes a novel approach to low-cost, accurate modeling of microwave structures using response features. Computational efficiency of the proposed method originates from the less nonlinear dependence of the feature points on the designable parameters of the structure of interest than conventionally used responses (e.g., S-parameters vs. frequency). Further decrease of the surrogate model setup cost is obtained by exploiting variable-fidelity EM simulations that are blended together using co-kriging interpolation. Comprehensive verification and comparisons with benchmark techniques is provided.

Index Terms — Microwave component modeling, computer-aided design, surrogates, space mapping, feature-based modeling, kriging, co-kriging.

I. Introduction

High-fidelity full-wave electromagnetic (EM) analysis allows for very accurate performance evaluation of microwave structures, however, usually at considerable computational expense, particularly for complex devices/circuits and when including interactions (EM couplings) with its environment. The cost of multiple EM simulations, as required in parametric optimization, uncertainty quantification, or yield-driven design (tolerance-aware design, design centering), may be prohibitive. Clearly, fast surrogate models are indispensable in carrying out such tasks in reasonable timeframe.

There are two basic options for surrogate model construction: approximation of sampled high-fidelity EM simulation data (popular methods: neural networks [1], kriging [2], support vector regression [3]) and physics-based modeling, i.e., appropriate correction of an underlying low-fidelity model such as an equivalent circuit (popular method: space mapping (SM) [4]). Approximation models are very fast but to ensure usable accuracy, they need large amounts of training data obtained through massive EM simulation. Physics-based surrogates require less training data and—due to the problem-specific knowledge embedded in the low-fidelity model—offer better generalization. However, they are less generic, more complex to implement, and their applicability is limited to cases when fast low-fidelity models are available (e.g., filters).

Reduction of the number of training points for approximation-based surrogates can be achieved by realizing the modeling process in an alternative representation of the system responses, where the dependence of the responses on the designable parameters is less nonlinear. This approach has been explored, e.g., in the SPRP technique [5] or in [6] for inverse modeling of filters. A modeling technique recently introduced in [7] utilizes a concept of feature points similar to SPRP but with considerably simpler implementation (achieved by abandoning the use of so-called reference designs [7]). Feature-based modeling has been demonstrated to ensure good accuracy using a fraction of the training points required by conventional methods [7].

In this work, we propose a variable-fidelity generalization of the feature-based modeling methodology. The surrogate is constructed using feature points extracted from EM simulation data at two discretization levels: coarse (low-fidelity model) and fine (high-fidelity model). High-fidelity model sampling is much sparser than the low-fidelity one. Both data sets are combined together using co-kriging [8]. Our approach is demonstrated using two microstrip filters. Comparative study indicates that the proposed methodology allows for considerable reduction of the surrogate model setup cost compared to both conventional approximation modeling (here, kriging interpolation) and feature-based modeling [7] without compromising its predictive power.

II. Variable-Fidelity Feature-Based Modeling

We will denote by $\boldsymbol{R}_f(\boldsymbol{x})$ the response vector of the expensive, high-fidelity EM-simulated model of the microwave structure of interest. $\boldsymbol{R}_f(\boldsymbol{x})$ may represent *S*-parameters at *m* chosen frequencies, ω_1 to ω_m, i.e., $\boldsymbol{R}_f(\boldsymbol{x}) = [R_f(\boldsymbol{x},\omega_1) \ldots R_f(\boldsymbol{x},\omega_m)]^T$; and $\boldsymbol{x}$ represents designable (e.g., geometry) parameters. The task is to construct a fast replacement model (surrogate) $\boldsymbol{R}_s$ of $\boldsymbol{R}_f$.

Let $X_T = \{\boldsymbol{x}^1, \boldsymbol{x}^2, \ldots, \boldsymbol{x}^N\}$ be the set of training samples. Conventional modeling methods aim at approximating the data pairs $\{\boldsymbol{x}^k, \boldsymbol{R}_f(\boldsymbol{x}^k)\}$ directly. Given the high nonlinearity of microwave device responses, particularly filters, it is a very challenging task that requires large data sets and which is virtually impossible in highly-dimensional design spaces.

Here, we propose a multi-fidelity feature-based modeling technique in which we exploit suitably selected feature points allocated on the response of the structure of interest. The feature points (cf. Fig. 1) may include points corresponding to specific response levels (e.g.,–10 dB, –3 dB), as well as those allocated in between fixed-level points (e.g., uniformly in frequency). As indicated in Fig. 2, dependence of the feature points on the design parameters is much less nonlinear than that of the original responses, and thus easier to model. Feature-based modeling was originally introduced in [7].

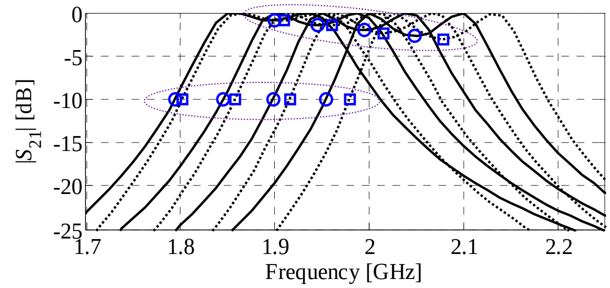

Fig. 1. Family of $|S_{21}|$ responses for a microstrip bandpass filter evaluated along a selected line segment $(1-t)\boldsymbol{x}^a + t\boldsymbol{x}^b$, $0 \le t \le 1$: high-fidelity model $\boldsymbol{R}_f$ (—) and low-fidelity model $\boldsymbol{R}_{cd}$ (····). Selected feature points and groups of corresponding points marked (o) for $\boldsymbol{R}_f$ and ( ) for $\boldsymbol{R}_{cd}$.

In this work, we utilize training data acquired from variable-fidelity simulations: sparsely-sampled $\boldsymbol{R}_f$ points $X_{Tf} = \{\boldsymbol{x}_f^1, \boldsymbol{x}_f^2, \ldots, \boldsymbol{x}_f^{Nf}\}$ and densely-sampled data obtained from coarse-discretization EM simulations (low-fidelity model $\boldsymbol{R}_{cd}$), $X_{Tc} = \{\boldsymbol{x}_c^1, \boldsymbol{x}_c^2, \ldots, \boldsymbol{x}_c^{Nc}\}$. Although $\boldsymbol{R}_{cd}$ and $\boldsymbol{R}_f$ are misaligned (cf. Fig. 1), they are also well correlated so that the initial surrogate model obtained from $\boldsymbol{R}_{cd}$ data can be enhanced using a few $\boldsymbol{R}_f$ points to construct the accurate, final surrogate model. Here, we use co-kriging [8] as a way of blending together the two data sets.

We use notation $\boldsymbol{f}_{k.f}^{\ j} = [\omega_{k.f}^{\ j}\ l_{k.f}^{\ j}]^T$, $j = 1, \ldots, K$, and $k = 1, \ldots, N_f$ to denote the jth feature point of $\boldsymbol{R}_f(\boldsymbol{x}_f^k)$, and $\boldsymbol{f}_{k.c}^{\ j} = [\omega_{k.c}^{\ j}\ l_{k.c}^{\ j}]^T$ to denote the jth feature point of $\boldsymbol{R}_{cd}(\boldsymbol{x}_c^k)$; $\omega_{k.f}^{\ j}$ and $l_{k.f}^{\ j}$ denote the frequency and magnitude (level) components of $\boldsymbol{f}_{k.f}^{\ j}$ (similarly for $\boldsymbol{f}_{k.c}^{\ j}$).

Multi-fidelity feature-based modeling is a two-step process. In the first step, we construct approximation surrogates $s_{\omega.j}(\boldsymbol{x})$ and $s_{l.j}(\boldsymbol{x})$, $j = 1, \ldots, K$, of the feature points. The surrogates utilize all N_f high-fidelity and N_c low-fidelity training points and their corresponding feature points $\{\boldsymbol{f}_{k.f}^{\ j}, \boldsymbol{f}_{k.f}^{\ j}, \ldots, \boldsymbol{f}_{Nf.f}^{\ j}\}$, and $\{\boldsymbol{f}_{k.c}^{\ j}, \boldsymbol{f}_{k.c}^{\ j}, \ldots, \boldsymbol{f}_{Nc.c}^{\ j}\}$, $j = 1, \ldots, K$. As mentioned before, the surrogates are created using co-kriging [8] (see Section III).

The multi-fidelity feature-based surrogate is defined as

$$\boldsymbol{R}_s(\boldsymbol{x}) = \left[R_s(\boldsymbol{x},\omega_1)\ \ldots\ R_s(\boldsymbol{x},\omega_m)\right]^T \tag{1}$$

with

$$R_s(\boldsymbol{x},\omega_j) = I(\Omega(\boldsymbol{x}), L(\boldsymbol{x}), \omega_j) \tag{2}$$

where $L(\boldsymbol{x}) = [s_{l.1}(\boldsymbol{x})\ \ldots\ s_{l.K}(\boldsymbol{x})]$ and $\Omega(\boldsymbol{x}) = [s_{\omega.1}(\boldsymbol{x})\ \ldots\ s_{\omega.K}(\boldsymbol{x})]$ are predicted feature point locations corresponding to the evaluation design $\boldsymbol{x}$. $I(\Omega,L,\omega)$ denotes a function that interpolates the level vector L and frequency vector Ω into the response at a given frequency ω_j.

Because $\omega_k^j(\boldsymbol{x})$ and $l_k^j(\boldsymbol{x})$ (i.e., frequencies and levels of the feature points) are less nonlinear than original responses $\boldsymbol{R}_f(\boldsymbol{x},\omega_j)$, a substantially smaller number of training points is necessary to ensure accurate modeling. Also, excellent correlation between $\boldsymbol{R}_{cd}$ and $\boldsymbol{R}_f$ (cf. Fig. 2) allows for further reduction of the surrogate model setup cost because a very limited number of $\boldsymbol{R}_f$ samples is sufficient to elevate the $\boldsymbol{R}_{cd}$-based kriging model to high-fidelity model accuracy through co-kriging.

III. Kriging Interpolation. Co-Kriging

Multi-fidelity feature-based modeling relies on kriging [2] and co-kriging [8] surrogates. Let $\boldsymbol{f}(X_{Tf})$ be the set of responses associated with the training set X_{Tf} (i.e., high-fidelity feature points $\boldsymbol{f}_{k.f}$ through $\boldsymbol{f}_{Nf.f}$). The kriging interpolant is given as

$$\boldsymbol{s}_{KR}(\boldsymbol{x}) = M\alpha + r(\boldsymbol{x}) \cdot \Psi^{-1} \cdot (\boldsymbol{f}(X_{Tf}) - F\alpha) \tag{3}$$

where M and F are Vandermonde matrices of the test point $\boldsymbol{x}$ and the base set X_{Tf}, respectively; α is determined by Generalized Least Squares (GLS), $r(\boldsymbol{x})$ is an $1{\times}N_f$ vector of correlations between the point $\boldsymbol{x}$ and the base set X_{Tf}, where the entries are $r_i(\boldsymbol{x}) = \psi(\boldsymbol{x},\boldsymbol{x}_f^i)$, and Ψ is a $N_f \times N_f$ correlation matrix, with the entries given by $\Psi_{i,j} = \psi(\boldsymbol{x}_{KR}^i, \boldsymbol{x}_{KR}^j)$. We use the exponential correlation function $\psi(\boldsymbol{x},\boldsymbol{x}') = \exp(\sum_{k=1,\ldots,n} -\theta_k|x_k - x'_k|)$. The regression function is constant, $F = [1\ \ldots\ 1]^T$ and $M = (1)$.

Co-kriging is a type of kriging where the $\boldsymbol{R}_f$ and $\boldsymbol{R}_{cd}$ model data are combined to enhance the prediction accuracy (cf. Fig. 3). Co-kriging is a two-step process: first a kriging model $\boldsymbol{s}_{KRc}$ of the coarse data $(X_{Tc},\boldsymbol{c}(X_{Tc}))$ is constructed and, on the residuals of the fine data $(X_{Tf},\boldsymbol{R}_d)$, a second kriging model $\boldsymbol{s}_{KRd}$ is applied, where $\boldsymbol{R}_d = \boldsymbol{f}(X_{Tf}) - \rho{\cdot}\boldsymbol{c}(X_{Tf})$; $\boldsymbol{c}(X_{Tf})$ can be approximated as $\boldsymbol{c}(X_{Tf}) \approx \boldsymbol{s}_{KRc}(X_{Tf})$. The co-kriging interpolant is defined as

$$\boldsymbol{s}_{CO}(\boldsymbol{x}) = M\alpha + r(\boldsymbol{x}) \cdot \Psi^{-1} \cdot (\boldsymbol{R}_d - F\alpha) \tag{4}$$

Definitions of M, F, $r(\boldsymbol{x})$ and Ψ can be found in [8].

IV. Verification Examples

The proposed modeling approach is verified using two examples of microstrip filters (Fig. 4): the fourth-order ring resonator bandpass filter [9], (Filter 1), and the microstrip bandpass filter with open stub inverter [10], (Filter 2). Design variables are $\boldsymbol{x} = [L_1\ L_2\ W_1\ S_1\ S_2\ d]^T$ (Filter 1), $\boldsymbol{x} = [L_1\ L_2\ L_3\ S_1\ S_2\ W_1\ W_2]^T$ (Filter 2), and $\boldsymbol{x} = [L_1\ L_2\ L_3\ S_1\ S_2\ W_1]^T$ (Filter 3).

The high-fidelity models of both filters are simulated in FEKO using 952 (10 minutes) and 432 triangular meshes (6 minutes), respectively.

The low-fidelity models are also simulated in FEKO but with coarser discretization: 174 meshes (simulation time 25 s) for Filter 1, and 112 meshes (simulation time 15 s) for Filter 1.

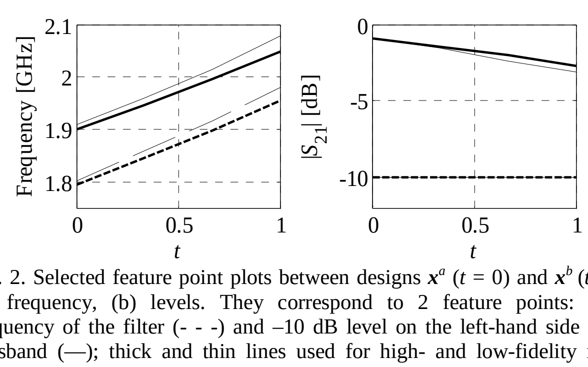

Fig. 2. Selected feature point plots between designs $\boldsymbol{x}^a$ ($t = 0$) and $\boldsymbol{x}^b$ ($t = 1$): (a) frequency, (b) levels. They correspond to 2 feature points: center frequency of the filter (- - -) and –10 dB level on the left-hand side of the passband (—); thick and thin lines used for high- and low-fidelity model feature points, respectively.

978-1-4799-8275-2/15/$31.00 ©2015 IEEE

Table I shows the accuracy verification using 100 random test designs and relative error measure $||\boldsymbol{R}_f(\boldsymbol{x}) - \boldsymbol{R}_s(\boldsymbol{x})||/||\boldsymbol{R}_f(\boldsymbol{x})||$ expressed in percent.

The multi-fidelity feature-based model is compared to feature-based surrogate [7] and direct kriging interpolation of high-fidelity data with different number of training points from 20 to 400. For all problems considered, the accuracy of the multi-fidelity feature-based surrogate is very good even for the smallest number of high-fidelity training samples (i.e., 20), and better than the accuracy of the benchmark methods for the corresponding number of training points. Figure 5 shows the high-fidelity and multi-fidelity feature-based model responses at selected test points.

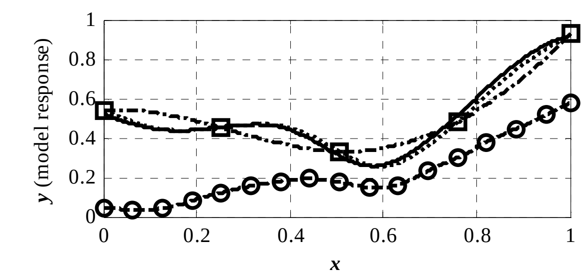

Fig. 3. Co-kriging concept: $\boldsymbol{R}_f$ model (—), $\boldsymbol{R}_c$ model (- - -), $\boldsymbol{R}_f$ model samples (□), $\boldsymbol{R}_c$ model samples (○). Kriging interpolation of $\boldsymbol{R}_f$ model samples (- · -) is not an adequate representation of the $\boldsymbol{R}_f$ model (limited data set). Co-kriging interpolation (····) of blended $\boldsymbol{R}_c$ and $\boldsymbol{R}_f$ data provides better accuracy at lower computational cost.

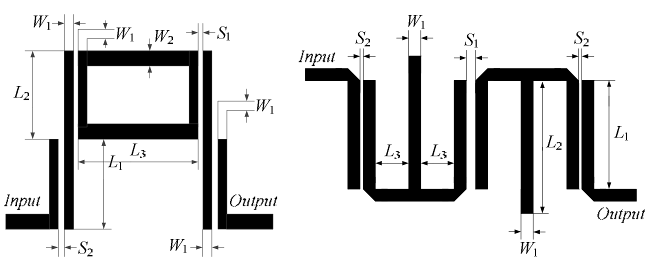

(a) (b)

Fig. 4. Filter structures used for feature-based modeling verification: (a) 4th-order ring resonator bandpass filter [9], (b) bandpass filter with open stub inverter [10].

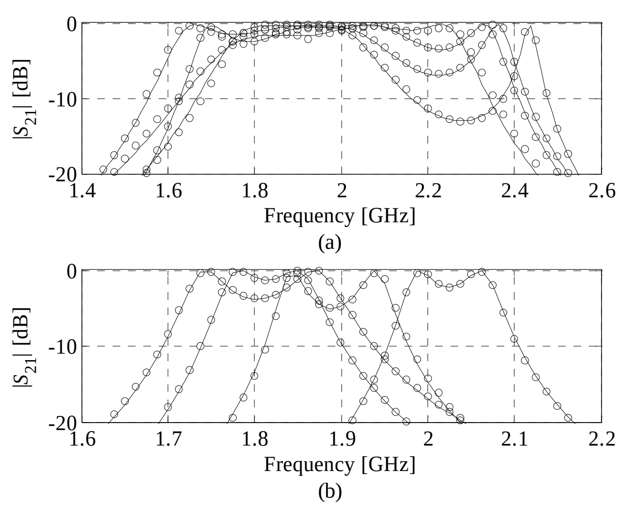

Fig. 5. High-fidelity (—) and multi-fidelity feature-based model (set up with 20 $\boldsymbol{R}_f$ and 200 $\boldsymbol{R}_{cd}$ points) (o) at the selected test designs for Filter 1 (a), and 2 (b).

TABLE I: MODELING RESULTS FOR FILTERS 1 AND 2

Filter	Modeling Method	Average Error				
		N^* = 20	N = 50	N = 100	N = 200	N = 400
1	Multi-Fidelity	3.7 %	1.5 %	1.3 %	1.2 %	1.2 %
	Feature-Based[$]	[28.3][&]	[58.3][&]	[108.3][&]	[208.3][&]	[408.3][&]
	Feature-Based[%]	11.6 %	5.1 %	3.8 %	3.6 %	2.5 %
	Direct Kriging[#]	13.5 %	7.8 %	6.3 %	4.6 %	3.6 %
2	Multi-Fidelity	0.7 %	0.6 %	0.5 %	0.45 %	0.4 %
	Feature-Based[$]	[28.3][&]	[58.3][&]	[108.3][&]	[208.3][&]	[408.3][&]
	Feature-Based[%]	7.5 %	2.4 %	1.2 %	0.7 %	0.6 %
	Direct Kriging[#]	11.6 %	8.8 %	6.1 %	4.8 %	3.1 %

[*] N stands for the number of training points.
[$] Multi-fidelity feature-based modeling of Section II using 200 $\boldsymbol{R}_{cd}$ samples.
[&] Numbers in brackets refer to the total model setup cost (including $\boldsymbol{R}_{cd}$ points).
[%] Feature-based modeling using the procedure of [7].
[#] Direct kriging interpolation of high-fidelity model $|S_{21}|$ responses.

V. CONCLUSION

A variable-fidelity feature-based technique for low-cost surrogate modeling of microwave structures is proposed. Realizing the modeling process through response features and utilizing both high- and low-fidelity EM simulation data allows for further reduction of the surrogate model setup cost compared with benchmark methods, including conventional kriging interpolation as well as feature-based modeling of high-fidelity data.

ACKNOWLEDGEMENTS

This work was supported in part by the Icelandic Centre for Research (RANNIS) Grant 130450051, by the Natural Sciences and Engineering Research Council of Canada under Grants RGPIN7239-11, STPGP447367-13, and by Bandler Corporation.

REFERENCES

[1] H. Kabir, Y. Wang, M. Yu and Q.J. Zhang, "Neural network inverse modeling and applications to microwave filter design," *IEEE Trans. Microwave Theory Tech.*, vol. 56, no. 4, pp. 867-879, Apr. 2008.

[2] N.V. Queipo, R.T. Haftka, W. Shyy, T. Goel, R. Vaidynathan, and P.K. Tucker, "Surrogate-based analysis and optimization," *Progress in Aerospace Sciences*, vol. 41, no. 1, pp. 1-28, Jan. 2005.

[3] L. Xia, J. Meng, R. Xu, B. Yan, and Y. Guo, "Modeling of 3-D vertical interconnect using support vector machine regression," *IEEE Microwave Wireless Comp. Lett.*, vol. 16, no. 12, pp. 639-641, Dec. 2006.

[4] J.W. Bandler, Q.S. Cheng, S.A. Dakroury, A.S. Mohamed, M.H. Bakr, K. Madsen, and J. Søndergaard, "Space mapping: the state of the art," *IEEE Trans. Microwave Theory Tech.*, vol. 52, no. 1, pp. 337-361, Jan. 2004.

[5] S. Koziel and L. Leifsson, "Generalized shape-preserving response prediction for accurate modeling of microwave structures," *IET Microwaves, Ant. Prop.*, vol. 6, no. 12, pp. 1332-1339, Sep. 2012.

[6] E. Menargues, S. Cogollos, V.E. Boria, B. Gimeno, and M. Guglielmi, "An efficient computer-aided design procedure for interpolating filter dimensions using least squares methods," *European Microwave Integrated Circuits Conf.*, pp. 250-253, 2012.

[7] S. Koziel, J.W. Bandler, and Q.S. Cheng, "Low-cost feature-based modeling of microwave structures," *Int. Microwave Symp.*, pp. 1-3, 2014.

[8] M.C. Kennedy and A. O'Hagan, "Predicting the output from complex computer code when fast approximations are available," *Biometrika*, vol. 87, pp. 1-13, 2000.

[9] M.K.M. Salleh, G. Pringent, O. Pigaglio, and R. Crampagne, "Quarter-wavelength side-coupled ring resonator for bandpass filters," *IEEE Trans. Microwave Theory Tech.*, vol. 56, no. 1, pp. 156-162, Jan. 2008.

[10] J.R. Lee, J.H. Cho, and S.W. Yun, "New compact bandpass filter using microstrip λ/4 resonators with open stub inverter," *IEEE Microwave and Guided Wave Letters*, vol. 10, no. 12, pp. 526-527, Dec. 2000.

978-1-4799-8275-2/15/$31.00 ©2015 IEEE